

Characterization and comparison of envelope detectors for wake-up sensor interfaces at audio frequencies

Marko Gazivoda

Faculty of Electrical Engineering and Computing, University of Zagreb
Zagreb, Croatia
marko.gazivoda@fer.hr

Dinko Oletić

Faculty of Electrical Engineering and Computing, University of Zagreb
Zagreb, Croatia
dinko.letic@fer.hr

Vedran Bilas

Faculty of Electrical Engineering and Computing, University of Zagreb
Zagreb, Croatia
vedran.bilas@fer.hr

Abstract— Ultra-low-power analog hardware interfaces are becoming often used for continuous monitoring of weak, rarely and randomly occurring (spurious) acoustic events. Detection often requires interfaces for analog-domain time-frequency decomposition. These interfaces most often have a generic structure incorporating the same processing blocks, such as amplification, filtering, rectification, quantization and rudimentary classification. A critical processing block of the wake-up sensor interface is the envelope detector. In this paper we select four envelope detector topologies and show simulation and measurement results of their key parameters for their application in wake-up sensor interfaces. The selected envelope detectors must have short transient times (< 100 ms), used to rectify weak input signals (under 10 mV) in the lower audio frequency range and have a low power consumption to make them applicable in wake-up sensor interfaces.

Keywords— *passive envelope detector, switched inductor envelope detector, weak-signal envelope detection*

I. INTRODUCTION

The research of low-power circuits is becoming more prominent because of their wide range of applications from IoT [1], communication systems [2], wake-up systems [3], detectors and monitoring systems [4], wearable and biomedical electronics [5] and many others. One of the most interesting applications of low-power circuits, that is providing solutions in many fields, are low-power wireless sensor networks. These networks require specific low-power, weak-signal embedded sensors most often used for continuous monitoring of spurious events, occurring randomly and rarely throughout the monitoring time.

Detection of spurious events based on time-frequency pattern recognition requires a set of signal processing operations and most sensor interfaces for this application have a structure incorporating processing blocks, such as amplification, filtering, rectification, quantization and rudimentary classification [6], [7]. The block schematic of the structure is shown in Fig. 1.

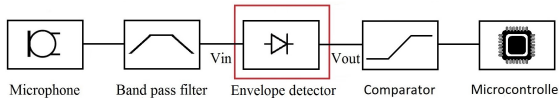


Fig. 1. An always-on wake-up sensor interface for spurious event detection based on time-frequency signal decomposition

The work of doctoral student Marko Gazivoda has been supported in part by the “Young researchers’ career development project – training of doctoral students” of the Croatian Science Foundation funded by the European Union from the European Social Fund.

This research has been supported in part by the U.S. Office of Naval Research Global under the project ONRG-NICOP-N62909-17-1-2160, AWAKE - Ultra low power wake-up interfaces for autonomous robotic sensor networks in sea/subsea environments, and partially by Croatian Science Foundation under the project IP-2016-06-8379, SENSIRIKA - Advanced sensor systems for precision irrigation in karst landscape.

A critical processing block of the wake-up sensor interface is the envelope detector, which is connected to the comparator input. The comparator must be able to respond quickly to the event and distinguish two events close in time. Therefore, the envelope detector must have a short rise and fall times (Fig. 2), estimated under 100 ms for the wanted application [7].

The comparator should also be able to distinguish as low levels of voltage as possible. So, the output headroom voltage (Fig. 2.) of the envelope detector should be at least 5 mV for the wake-up sensor interface application [7].

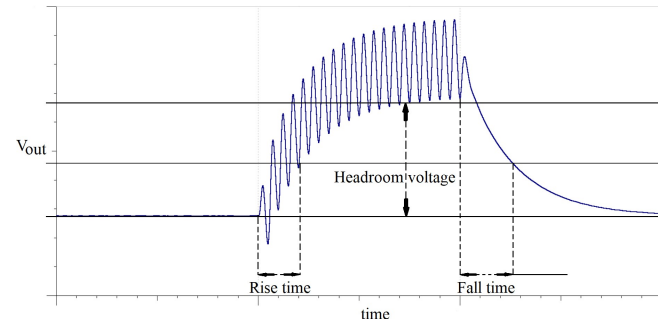


Fig. 2. A graphic representation of the values of interest in simulation and measurement – headroom voltage, rise and fall time

There are several other demands on wake-up sensor interface envelope detectors stemming from their application – working with input voltages under the diode threshold and having a low power consumption.

In this paper we will focus on envelope detectors operating in the lower audio frequency range, as this frequency range is rich in easily extracted useful information about the phenomena of interest. A lot of work has recently been done in development of appropriate envelope detection solutions. In [8] the authors present a fully passive envelope detector that works with input signals as low as 100 mV at frequencies from DC to 100 MHz. In [9] a low-power envelope detector is presented with power consumption of just 10 nW, operational with an input as low as 50 mV at 50 Hz. In [10] an envelope detector with around 100 nW power consumption is presented, that can work with input signals over 100 mV at a low frequency of only 4 Hz. It should be noted that the envelope detectors presented in [8]–[10] are integrated, unlike the prototypes in this paper, which are made of commercially available components.

In vibration energy harvesting the problem of low generated voltages (under the diode threshold) is solved by utilizing the concept of envelope detectors with a switched inductor, such as SSHI (synchronous switched harvester on inductor) to increase the envelope detector’s efficiency [11], [12].

In this paper we characterize and compare four envelope detector topologies and show simulation and experimental results of key parameters for their application in low-power embedded wake-up sensor interfaces. The selected envelope detector topologies are: passive single-diode half-wave envelope detector, passive two-diode half-wave voltage doubler (Graeischer circuit), active two-diode half-wave voltage doubler utilizing an operational amplifier and an active full-wave envelope detector utilizing a switched inductor (switched by an electrical switch driven by an oscillator).

This paper is organized as follows: Section II presents a simulation study of the envelope detectors, showing the simulation models and results, Section III presents the experimental setup and results measured using the developed prototypes, Section IV presents a summary comparison of the envelope detectors and Section V presents the concluding remarks of the paper, along with possible future work.

II. SIMULATION STUDY

The goals of the simulation study were the selection of passive and active components for envelope detector realization and preliminary insight into parameters of interest (headroom voltage, rise and fall time). The presented simulations were done using TINA-TI, a Texas Instruments SPICE-based analog simulator.

A. Simulation models and setup

The simulation models are shown in Fig 3. a) through d).

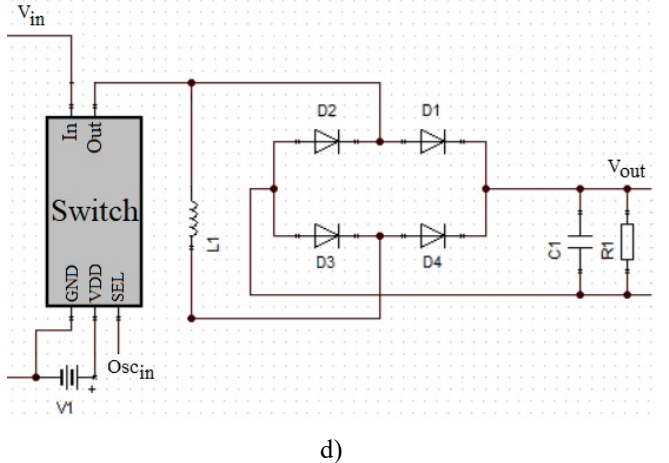
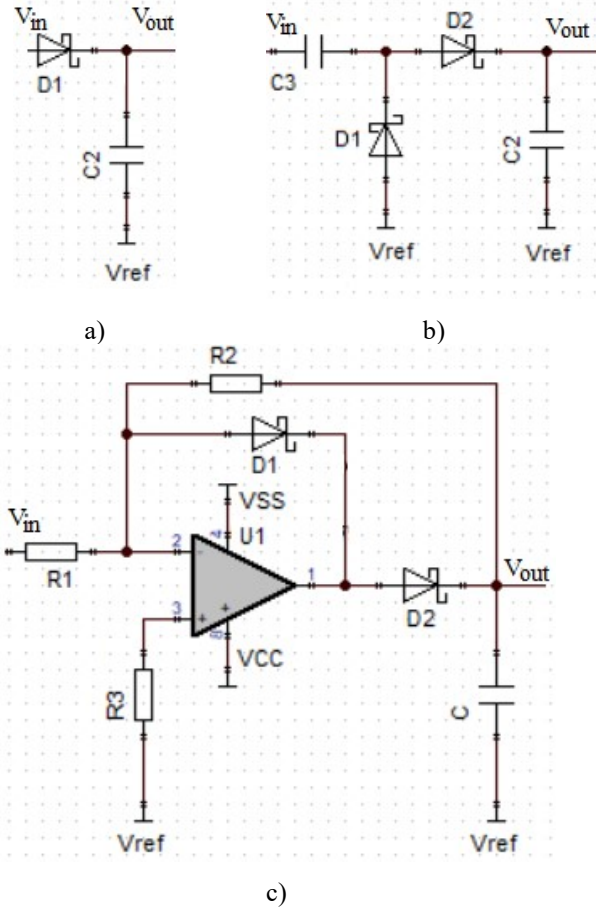


Fig. 3. Envelope detector topologies: a) passive single-diode half-wave envelope detector, b) passive two-diode half-wave voltage doubler (Graeischer circuit), c) active two-diode half-wave voltage doubler utilizing an operational amplifier and d) active full-wave envelope detector utilizing a switched inductor

The envelope detector input signal was a gated sinusoidal signal because that allows both transient times to be measured. The duration of the sinusoidal signal was set to 1.5 s. The set input voltages for all envelope detectors were 1 mV, 2 mV, 3 mV, 5 mV, 7 mV and 10 mV and the input frequencies 128 Hz, 256 Hz and 512 Hz for the switched inductor envelope detector and 200 Hz, 500 Hz and 1000 Hz for the other three topologies. In the simulation model for the switched inductor envelope detector, the electrical switch is triggered by a 256 Hz oscillator (not synchronized with the input signal). The input signals and the oscillator signal (Fig. 3.d)) are made in MATLAB and imported to the TINA-TI simulator.

The load capacitor values were set to 3.3 nF, 6.8 nF, 10 nF, 15 nF, 22 nF, 33 nF, 100 nF, 350 nF and 1 μ F. In all the simulations several diodes' performances were compared. In addition, for the active envelope detector with the operational amplifier two amplifiers were compared – the Texas Instruments' OPA379 and Microchip's MCP6141 and for the active envelope detector with the switched inductor the three switches were compared – TPS22916, TPS22976 and TPS22860 from Texas Instruments.

For the active envelope detector utilizing an operational amplifier several values of resistors were tested. Simulations of the switched inductor envelope detector were done with three inductor values: 1 mH, 10 mH and 100 mH.

B. Simulation results

Table I. shows the simulation results for the headroom voltages, rise and fall times of the four proposed envelope detector topologies (for the full range of load capacitor values). Simulation results were processed using MATLAB.

From the simulation results Avago Technology's HSMS-282x diodes were chosen for all the envelope detectors as they allowed for the best headroom voltages and a relatively flat frequency response in the frequency range of interest. For the active envelope detector utilizing the operational amplifier the MCP6141 amplifier was chosen because of its slightly higher headroom voltages and shorter transient times (and lower declared power consumption). For the switched inductor envelope detector, the TPS22860 switch was chosen as it gave a far higher headroom voltage.

TABLE I. SELECTED ENVELOPE DETECTORS SUMMARY COMPARISON

single-diode passive envelope detector			
Input signal frequency (Hz)	Headroom (mV)	Rise time (ms)	Fall time (ms)
200	< 2.84	14.86 – 50.29	13.30 – 41.01
500	< 3.16	7.95 – 47.87	6.35 – 33.85
1000	< 2.82	6.05 – 36.12	5.08 – 34.86
two-diode passive voltage doubler			
Input signal frequency (Hz)	Headroom (mV)	Rise time (ms)	Fall time (ms)
200	< 5.25	19.66 – 79.87	16.41 – 89.92
500	< 5.98	11.83 – 52.03	10.77 – 77.28
1000	< 5.46	9.96 – 45.75	8.69 – 73.11
active voltage doubler utilizing an operational amplifier			
Input signal frequency (Hz)	Headroom (mV)	Rise time (ms)	Fall time (ms)
200	< 80.69	2.50 – 5.33	2.67 – 7.61
500	< 78.32	1.20 – 3.62	2.33 – 6.15
1000	< 70.23	1.60 – 4.4	1.61 – 14.23
active envelope detector utilizing a switched inductor			
Input signal frequency (Hz)	Headroom (mV)	Rise time (ms)	Fall time (ms)
128	< 8.53	20.07 – 238.95	27.32 – 251.34
256	< 8.17	20.09 – 238.80	27.36 – 246.80
512	–	–	–

The simulation results also pointed to the fact that larger load capacitor values (100 nF, 350 nF and 1 μ F) should be used for the switched inductor envelope detector to reduce the ripple caused by its impulse operation (high pulse values of currents charging the capacitor), which leads to this topology having longer transient times. The remaining topologies should use the lower capacitor values (< 100 nF).

The chosen values for the resistors in the active topology utilizing the operational amplifier were $R_1 = 200 \text{ k}\Omega$, $R_2 = 1 \text{ M}\Omega$ and $R_3 = 100 \text{ k}\Omega$ and the 100 mH inductor value was chosen in the switched inductor topology, because it gave the highest output voltages with the same input current.

Simulation results have also shown some envelope detectors to be unusable at certain input voltages (passive single-diode envelope detector with lower input voltages), or frequencies (switched inductor envelope detector at 512 Hz).

III. EXPERIMENTAL STUDY

Prototypes of each envelope detector were made in order to acquire experimental measurement data. In the following subsections the measurement setup and procedure are described, and experimental results presented.

The goal of these measurements was to characterize and compare the four proposed envelope detector topologies from the aspects of headroom voltage, rise time, fall time and power consumption, in order to determine their applicability in a wake-up sensor interface.

A. Experimental setup

The block diagram and a photograph of the measurement setup can be seen in Fig. 8. and Fig. 9. respectively. The measurement setup consisted of a waveform generator (Keysight 33500B) connected to the input of the prototype envelope detector. The output voltage was acquired by a

National Instruments data acquisition card (NI USB-6211) connected to a PC. The switches were powered by a DC power supply (Rigol DP832) and the supply current measured by a multimeter (Fluke 45).

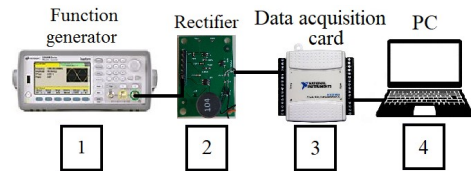


Fig. 4. Block diagram of the measurement setup: a function generator (1), the envelope detector PCB (2) a data acquisition card (3) connected to a PC (4).

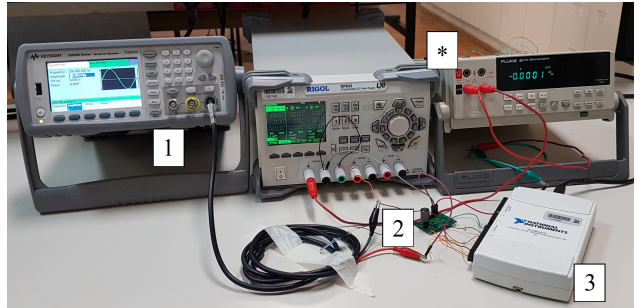


Fig. 5. A photograph of the measurement setup. 1) Keysight 33500B waveform generator, 2) envelope detector prototype, 3) NI USB-6211 data acquisition card, *) Power supply (Rigol DP832) and a multimeter for supply current measurement (Fluke 45).

B. Experimental procedure

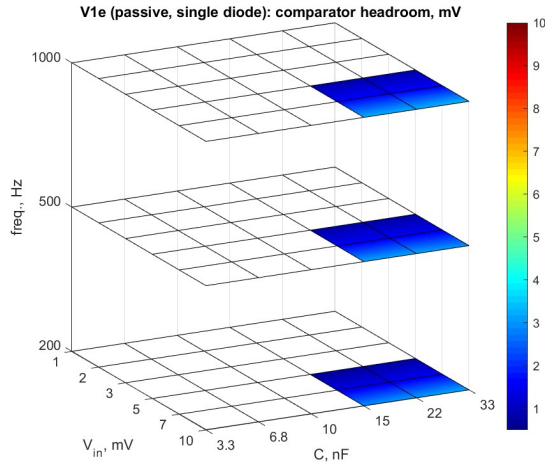
The power consumption of the envelope detectors, with a set supply voltage of 1.8 V, was measured by measuring the supply current using a multimeter (Fluke 45). The remaining three parameters were measured simultaneously, by setting the input voltage at the envelope detector input using a waveform generator and measuring the characteristics of the output voltage (Fig. 2.) acquired by a data acquisition card.

The measurements done at three frequencies: 128 Hz, 256 Hz and 512 Hz for the switched inductor envelope detector (switching was controlled by a 256 Hz oscillator) and 200 Hz, 500 Hz and 1000 Hz for the remaining three envelope detectors. For all frequencies six input signal peak-to-peak voltages were set: 1 mV, 2 mV, 3 mV, 5 mV, 7 mV and 10 mV.

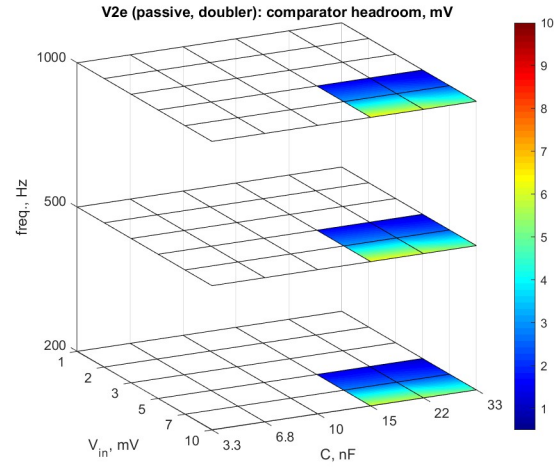
The measurements for the switched inductor envelope detector were done with three capacitors: 100 nF, 350 nF and 1 μ F. The measurements for the two passive envelope detectors were also done with three capacitors: 10 nF, 15 nF and 33 nF. The measurements for the active envelope detector with an operational amplifier were done with four capacitors: 3.3 nF, 6.8 nF, 10 nF and 15 nF.

C. Experimental results

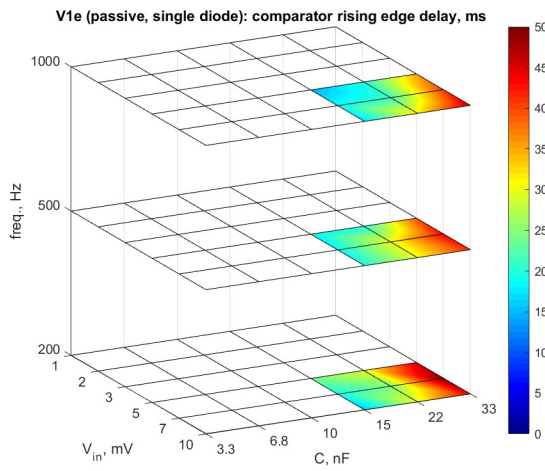
The obtained experimental results are shown in Fig. 6-9., one for each of the selected envelope detectors, showing the headroom voltage (a), rise time (b) and fall time (c). The results were processed and presented using MATLAB.



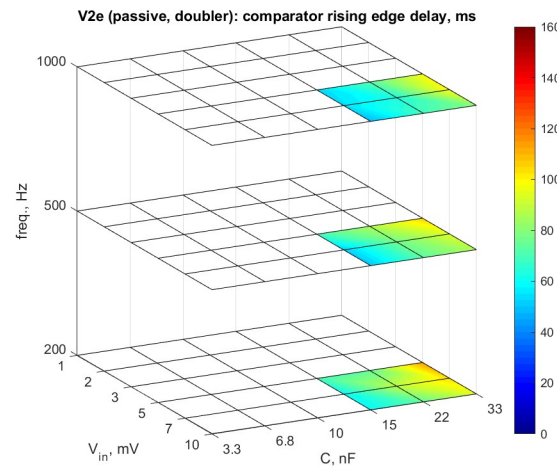
a)



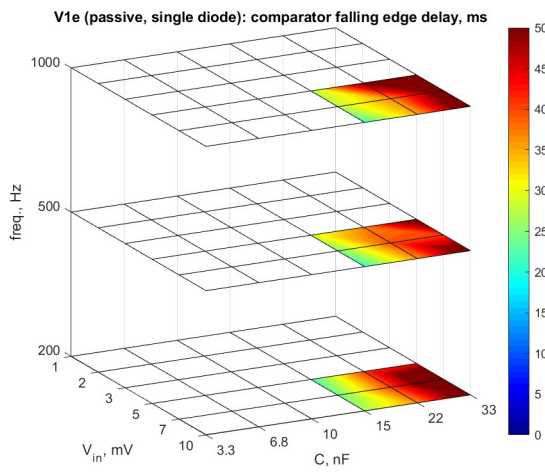
a)



b)

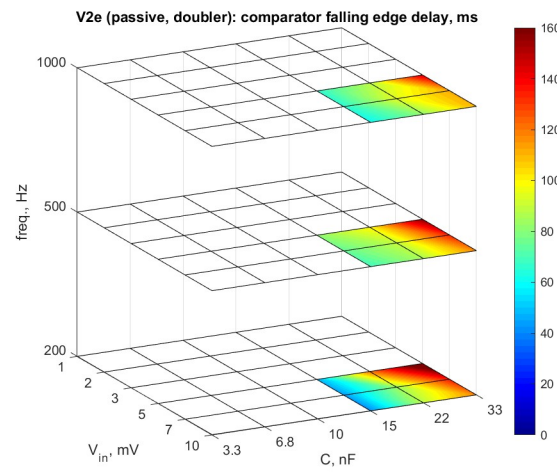


b)



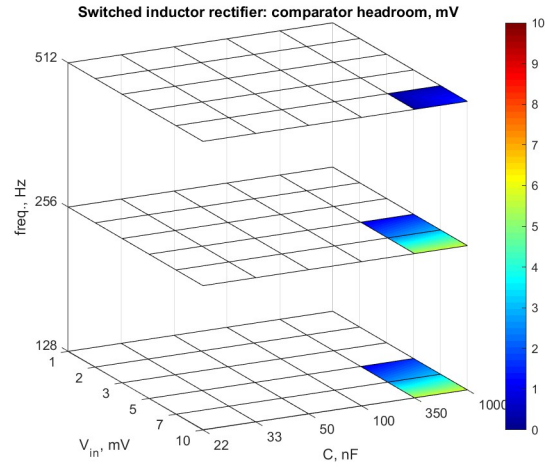
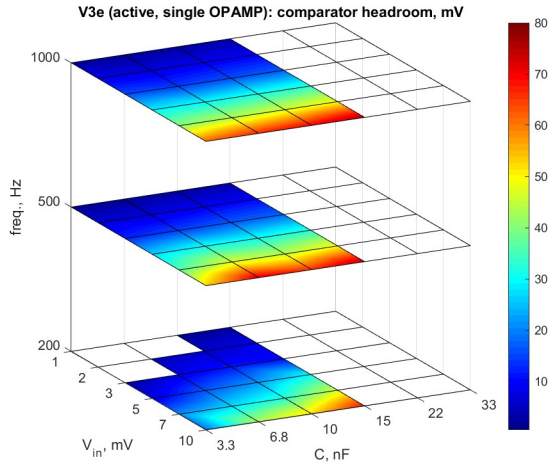
c)

Fig. 6. Experimental results for the passive single diode half-wave envelope detector: a) headroom voltage, b) rise time c) fall time

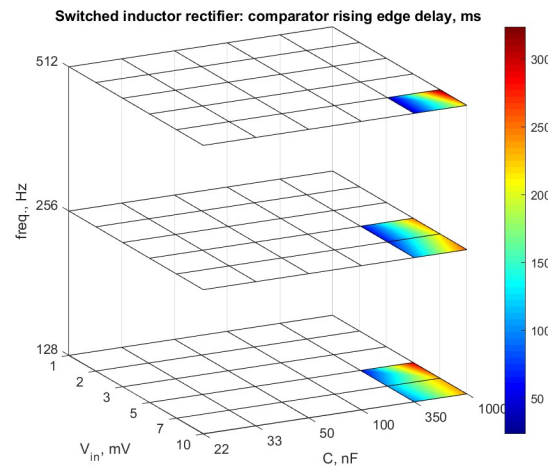
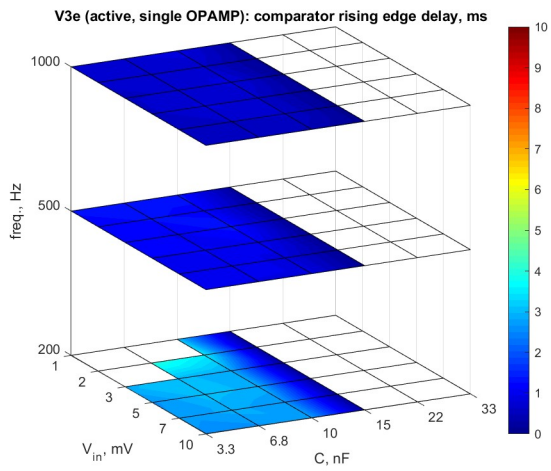


c)

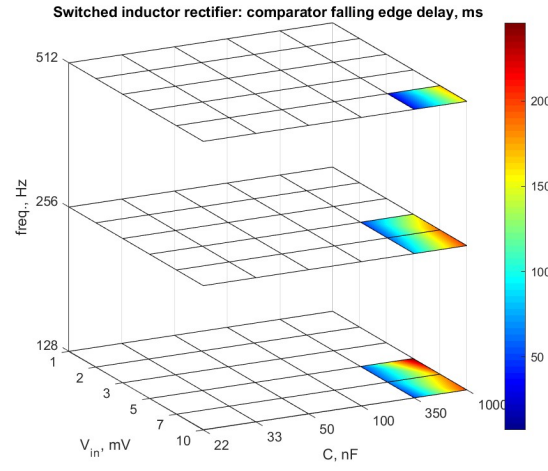
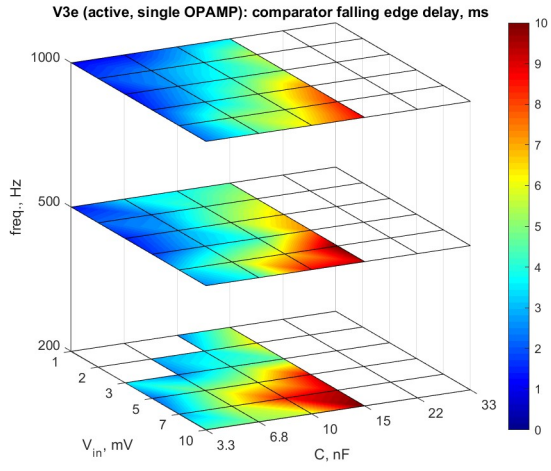
Fig. 7. Experimental results for the passive two-diode half-wave voltage doubler (Greinacher circuit): a) headroom voltage, b) rise time c) fall time



a)



b)



c)

Fig. 8. Experimental results for the active two-diode half-wave voltage doubler utilizing an MCP6141 operational amplifier: a) headroom voltage, b) rise time c) fall time

Measurement results for the passive single-diode envelope detector confirm the simulation results and show the headroom voltage to be too low (<2 mV).

Fig. 9. Experimental results for the active full-wave envelope detector utilizing a 100 mH switched inductor: a) headroom voltage, b) rise time c) fall time

The results for the passive voltage doubler show that the headroom voltage is high enough (>5 mV). However, this envelope detector exhibits longer fall times (> 100 ms).

This active envelope detector with the MCP6141 operational amplifier achieves very high headroom voltages (> 70 mV) and short transient times (~ 10 ms). Its power consumption of $1.44 \mu\text{W}$ stems from its operational amplifier.

The switched inductor envelope detector utilizing a TPS22860 switch and SiT1569 oscillator shows high enough headroom voltage (> 5 mV), but long rise and fall times (around 250 ms). The relatively high power consumption of $3.42 \mu\text{W}$ of this envelope detector stems from the oscillator and electrical switch.

Table II. shows a summary comparison of the four selected envelope detectors.

TABLE II. PROPOSED ENVELOPE DETECTORS SUMMARY COMPARISON

Topology	Power consumption	Headroom voltage	Transition times
one-diode passive	–	< 2 mV	med., < 50 ms
two-diode passive	–	~ 5.5 mV	long, > 100 ms
active, op. amp.	$1.44 \mu\text{W}$	~ 70 mV	short, < 10 ms
active, switched L	$3.42 \mu\text{W}$	~ 5.5 mV	long, > 200 ms

IV. CONCLUSION

In this paper we presented a characterization and comparison of four candidate envelope detector topologies for application in wake-up sensor interfaces for lower audio frequencies. From the presented simulation and experimental characterization and comparison data the active half wave voltage doubler utilizing an MCP6141 operational amplifier can be used for application in a wake-up sensor interface and outperforms the switched inductor envelope detector in the selected topology with the selected components.

In future work the switched inductor envelope detector topology will be explored further to devise ways of reducing its power consumption and shortening its transient times.

REFERENCES

- [1] M. Alioto, *IoT: Bird's Eye View, Megatrends and Perspectives*. 2017.
- [2] H. Fuketa, S. O'uchi, and T. Matsukawa, "A 0.3-V 1- μW Super-Regenerative Ultrasound Wake-Up Receiver with Power Scalability," *IEEE Trans. Circuits Syst. II Express Briefs*, vol. 64, no. 9, pp. 1027–1031, 2017.
- [3] M. Gazivoda, D. Oletic, C. Trigona, and V. Bilas, "Measurement of Weak Signal Energy at Acoustic Frequencies by using RMSHI as a Passive Conditioning Circuit," *I2MTC 2019 - 2019 IEEE Int. Instrum. Meas. Technol. Conf. Proc.*, pp. 1735–1739., 2019.
- [4] P. Mayer, M. Magno, and L. Benini, "Self-Sustaining Acoustic Sensor with Programmable Pattern Recognition for Underwater Monitoring," *IEEE Trans. Instrum. Meas.*, vol. 68, no. 7, pp. 2346–2355, 2019.
- [5] D. Oletic and V. Bilas, "Energy-efficient respiratory sounds sensing for personal mobile asthma monitoring," *IEEE Sens. J.*, vol. 16, no. 23, pp. 8295–8303, 2016.
- [6] N. Goux and F. Badets, "Review on event-driven wake-up sensors for ultra-low power time-domain design," *Midwest Symp. Circuits Syst.*, vol. 2018-Augus, pp. 554–557, 2019.
- [7] D. Oletic, V. Bilas, M. Magno, N. Felber, and L. Benini, "Low-power multichannel spectro-temporal feature extraction circuit for audio pattern wake-up," *2016 Des. Autom. Test Eur. Conf. Exhib.*, pp. 355–360, 2016.
- [8] R. S. Suri, N. T. Tasneem, and I. Mahbub, "Low-power highly efficient voltage-boosting rectifier for wide-band inductively-coupled power telemetry," *2019 United States Natl. Comm. URSI Natl. Radio Sci. Meet. Usn. NRSM 2019*, no. 1, pp. 1–2, 2019.
- [9] J. Gak, M. Miguez, E. Alvarez, and A. Arnaud, "Integrated ultra-low power precision rectifiers for implantable medical devices," *2019 Argentine Conf. Electron. CAE 2019*, pp. 27–30, 2019.
- [10] K. G. Sun, K. Choi, and T. N. Jackson, "Low-power double-gate ZnO TFT active rectifier," *IEEE Electron Device Lett.*, vol. 37, no. 4, pp. 426–428, 2016.
- [11] S. Du, G. A. J. Amaralunga, and A. A. Seshia, "A Cold-Startup SSHI Rectifier for Piezoelectric Energy Harvesters with Increased Open-Circuit Voltage," *IEEE Trans. Power Electron.*, vol. 34, no. 1, pp. 263–274, 2019.
- [12] X. Li and Y. Sun, "An SSHI Rectifier for Triboelectric Energy Harvesting," *IEEE Trans. Power Electron.*, vol. 8993, no. c, pp. 1–15, 2019.